Applied Materials Today 27 (2022) 101414

Contents lists available at ScienceDirect

Applied Materials Today

journal homepage: www.elsevier.com/locate/apmt

Programmable and reconfigurable hygro-thermo morphing materials with multifunctional shape transformation

Qinyu Li[a,1], Rujie Sun[b,1], Antoine Le Duigou[c], Jianglong Guo[d], Jonathan Rossiter[e], Liwu Liu[f], Jinsong Leng[g,*], Fabrizio Scarpa[a,*]

[a] Bristol Composites Institute, University of Bristol, Bristol BS8 1TR, UK
[b] Department of Materials, Department of Bioengineering and Institute of Biomedical Engineering, Imperial College London, London, UK
[c] Polymer and Composites, UMR CNRS 6027, IRDL,Université Bretagne Sud, Lorient F-56100, France
[d] School of Science, Harbin Institute of Technology (Shenzhen), Shenzhen, PR China
[e] SoftLab, Bristol Robotics Laboratory, University of Bristol, Bristol, UK
[f] Department of Astronautical Science and Mechanics, Harbin Institute of Technology (HIT), P.O. Box 301, No. 92 West Dazhi Street, Harbin 150001, PR China
[g] National Key Laboratory of Science and Technology On Advanced Composites in Special Environments, Harbin Institute of Technology (HIT), No.2 Yikuang Street, P.O. Box 3011, Harbin 150080, PR China

ARTICLE INFO

Article history:
Received 12 November 2021
Revised 12 January 2022
Accepted 2 February 2022

Keywords:
Hygromorph
Shape memory polymers
Programmable
Reconfigurable

ABSTRACT

Humidity responsive materials are increasingly attracting significant interest for soft robotics and deployable structures. Their shape-changing behavior is based on differential hygroscopic characteristics of the single components of their microscopic architecture. Although existing moisture-induced materials achieve morphing in various humidity conditions, practical operational environments involve the presence of uncontrolled humidity regimes, which restrict those materials to reach broad ranges of shapes. Here we describe programmable and reconfigurable composite materials based on natural fibres and shape memory polymers that extend the current one-to-one relation between external humidity and final actuated shape. The heating of flexible polymer networks permits to program the architecture of the natural fibres flax reinforcements and their spatial distribution within the composite, when a moisture gradient is present. Once cooled, the programmed materials create new sets of different shapes, even when exposed to the same humidity conditions. These multifunctional biobased materials also show large stiffness (>13 GPa) that make them suitable for structural load-bearing applications. New multifunctional shape transformations capabilities of these bio-based hygro-thermo composites are demonstrated in a bio-robotic grasping hand and a bio-frame for electro-adhesive gripping. These examples show the full functionality, structural integrity, programmability and remarkable mechanical properties of our multifunctional hygromorph biocomposites.

1. Introduction

Reconfigurable solids are smart materials that can be programmed and transformed using external stimuli such as - amongst others – heat [1], light [2], water [3], electricity [4], and magnetic fields [5]. When used to design actuators and morphing (shape-changing) structures, those materials can provide bending [6], twisting [7] and folding [8]. External devices/power inputs are however necessary to provide the relative stimulus. Piezoelectrics rely on electronic integration [9,10]; electroactive polymers are controlled by external electric fields [11,12], while pneumatics and hydraulics are based on the dynamic reconfiguration of fluids [13,14]. Shape memory materials (polymers and alloys) typically require a second stimulus to enable programming [15,16] such as being immersed in hot air/gas flow [6], hot liquid [17] or being actuated by electrothermal films [18]. The development of most stimulus-responsive materials is limited to the laboratory stage because the operational conditions to actuate those materials are not practical in many engineering applications (i.e., very hot fluids [18,19]. Pneumatics [15], and hydraulics) [16]. Commonly used methods to provide stimulus are mainly based on the integration of electrics/electronics via complex wiring and use of electrodes; this increases the complexity and failure in the structural assemblies present, for example, in conventional robotics. Thermal fields provided by hot fluids are not easy to handle during operations, and their working may be affected by or influence the pres-

* Corresponding authors.
E-mail addresses: lengjs@hit.edu.cn (J. Leng), F.Scarpa@bristol.ac.uk (F. Scarpa).
[1] Qinyu Li and Rujie Sun contributed equally to this work.

https://doi.org/10.1016/j.apmt.2022.101414
2352-9407/

ence of other connected subsystems. Pneumatics and hydraulics rely on the presence of pumps and fluid/air transformers, which are in general large and heavy. The extra devices required to provide a stimulus for the actuation may limit the feasibility of cost-effective practical industrial applications involving shape change and morphing.

The stimulus provided by the surrounding environment is ideal to reduce the need for external power/actuation devices. Moreover, autonomous materials tend to actuate most effectively when their response is pre-programmed to respond to changes of the surrounding environment. Higher energy density stimuli such as continuous current [11–14,20], pneumatics [15], hydraulics [16], and high temperatures [18,20] are difficult to obtain in practical working environments. In contrast, mass transfer is an efficient manner to generate response in autonomous materials. Existing examples are limited; those include hydrogels that store 0.1 M NaCl solution and actuate via deionized water [19], autonomous pinecone robots for outdoor natural environments [20] and hygromorph biocomposites as hinges of deployable structures to trigger autonomous self-snapping in water [21]. These moisture-responsive materials perform shape change in an autonomous way if the humidity of the surrounding environment is different from the one of stored conditions. These autonomous materials also possess a one-to-one only relationship between their mass content and their changing shapes. In other words, the expected shape change is only shown within a specific humidity environment. However, this does not provide a broad set of autonomous actuations and morphing conditions within various relative humidity situations.

To tackle the issue, we present here a novel class of active hygro-thermo morphing shape-changing composite (HyTemC) made of natural fibres and shape memory polymers (SMPs) that exhibits multifunctional shape transformations. The HyTemC enables to program the geometry and the effective spatial distribution of internal natural fibres (flax, in our case) used as reinforcement. This functionality allows to build up new sets of shapes at various humidity conditions. The programmable HyTemC provides multifunctional, autonomous, repeatable, and reversible shape transformations, while also locking the actuator made with these biocomposites on the morphed shapes. This novel HyTemC concept will first be explored through the measurements and analysis of the longitudinal curvature of actuated HyTemC-made beams. The curvatures will be assessed as a function of various programming and actuating cycles that are activated by combinations of moisture and temperature. We will also provide two examples of applications illustrating the potential of the new thermal/moisture absorption functionality: one application is related to a bio-robotic grasping hand with five fingers, the other to an electro adhesive gripper with smart bio-frames. These two applications involve the initial design of the final actuated shapes at specific operational relative humidity values, followed by programming steps of the material based on the initial set conditions. The two test cases feature autonomous actuations stimulated by the operational surrounding environment, without the use of any external device. The bio-robotic grasping hand can lift a ball more than 8 times its own weight in both water and 50% relative humidity (RH) at room temperature, while the electro adhesive gripper conformally adapts to different object shapes at room humidity conditions, providing sufficient adhesion to enable the lift.

2. Materials and mechanisms

2.1. The HyTemC concept – a biobased composite material with intrinsic augmented programmability

Symmetric unidirectional natural fibres composites are likely to swell significantly along the radial direction of the fibres when absorbing moisture but undergo little expansion along the fibres longitudinal direction [3,21] (2.83% and -0.04% respectively in our case, from 0% RH to immersed conditions - see Fig. S1 c of the Supplementary Information). When the fibres are embedded in a SMP matrix, the hygroscopic expansion along the radial direction of the fibres at room temperature is still remarkable, but it decreases considerably when heating over the glass transition temperature (T_g) - from 2.83 to 0.78%, as also shown in Fig. S1 c. After cooling down to room temperature, the SMP/natural fibre composite contains the same the moisture content (MC), but completely different hygroscopic expansions from direct absorption, which allows matter programming features. Moisture-responsive hydrogels also present different significantly swelling ratios (9.2) at room temperature, but only 1.5 over T_g temperature [22].

The HyTemC here has an internal asymmetric microstructure inspired by pinecone scales and consists of stiff passive and soft active layers. The passive layers have a low axial swelling along the longitudinal (0°) direction, given by the flax fibres embedded in the polymer matrix. The softer active layers possess a high swelling achieved by the transversally (90°) placed flax fibres. Shape change is controlled by the large difference in swelling or shrinking between the active and the passive layers - 2.83 and -0.04% from 0% RH to immersion**.** The samples developed here are marked as $[0_m 90_n]$, meaning that the bilayer microstructure architecture has m laminas in the longitudinal direction as passive layers, and n lamina along the transverse direction as active layers. A direct correlation exists between the shapes of beams made with standard hygromorph solids and their MC. This correlation can be predicted by using a modified version of the Timoshenko equation for slender asymmetric beams [3]. As a significant departure from current hygromorph composites [3,21], the HyTemC makes however use of shape memory polymers that create programmability of the internal geometry of the flax fibres bundles and their microscale distribution. This allows to build a new mapping between actuated shapes and humidity conditions (see Fig. 1a). Although the geometry of the fibres architecture still changes considerably from 0% RH to immersion above T_g, the overall expansion of the active layers decreases sharply from 2.83 to 0.78%. Fibres expand or shrink based on their inner moisture content, but the SMP matrix helps to maintain the original overall shape of the composite. The expansion and/or shrinkage of the fibres generate new modified spatial distributions/architectures of the fibres bundles themselves, as well as providing local tension or compression on the matrix. At macro level, the compensating effects between fibres and matrix deformations lead to hygromorph composites with negligible changes of their hygroscopic properties. Besides the reduced expansion of the active layers, the release of stress from the flexible epoxy SMP chains when heating above T_g between the active and passive layers produces nearly flat shapes with negligible dimensional changes, even when extensive moisture content transfers are present. These features allow to program the biobased material. The HyTemC is programmed here by heating above the T_g and by controlling the inner moisture content by absorption or desorption. When the programming is finished, the biocomposite is cooled down to room temperature. Our programmed HyTemC example ($[0_2 90_6]$) provides a broad set of actuated shapes responding to different humidity conditions (see Fig. 1b). The programming is performed here at 3.26% inner MC (50% external RH) and 22.68% MC (with the composite in full immersion).

Matrix selection is quite critical for both the actuation at various RH conditions, but also for programming via the variation of the positions of the fibres. The ideal matrix should (a) provide enough stiffness at room temperature for acceptable mechanical performance during actuation; (b) have proper viscoelastic properties above T_g for local tensile or compressive load transfers when the individual fibres shrink or swell (i.e., in the case of our SMP

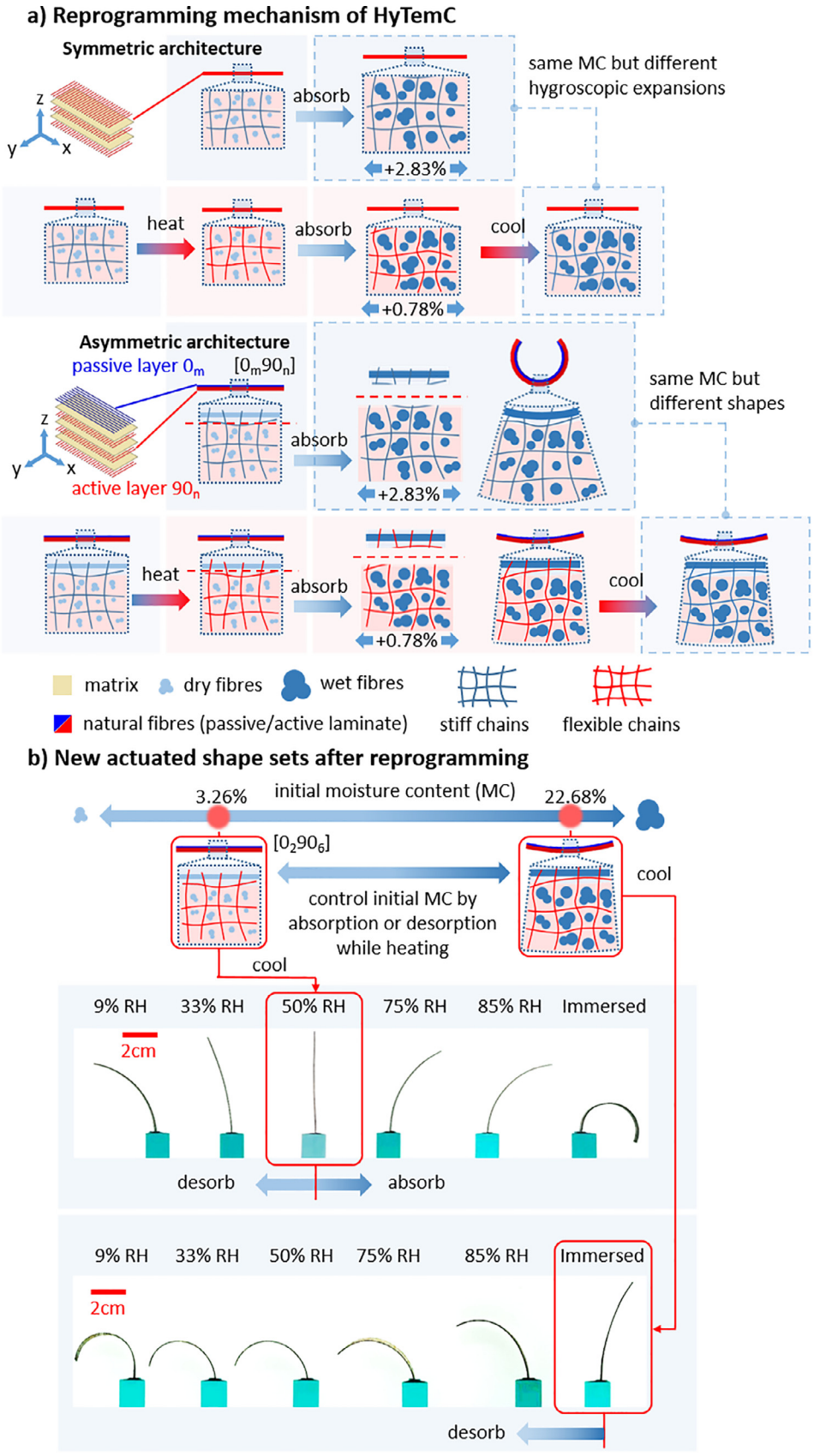

Fig. 1. (a) The HyTemC consists of stiff and low axial swelling passive layers, as well as soft and radial swelling active layers. Flax fibres tape and resin film are stacked and cured into a $[0_m 90_n]$ composite. The geometry of the flax fibres varies with the internal moisture content, which contributes to a very large differential hygroexpansion between the active and passive layers in the longitudal (x) direction -2.83% and -0.04% from 0% RH to immersion. Large bending therefore occurs when a moisture gradient exists. Temperature is introduced to break the usual one-to-one relationship between changing shapes and inner MC. The SMP epoxy matrix used here tends to keep the original shape of the composite when the fibres swell or shrink (only 0.78% expansion compared to 2.83% of the standard polymer). The significant reduction of the expansion of the active layers and the release of stresses between layers promote negligible shape changes, although considerable variations of the inner MC occur. The mechanism behind the programming functionality of the HyTemC consists therefore in the control of the fibres geometry/distribution by absorption and desorption, while keeping the whole composite architectures and shapes nearly flat. Composites with nearly flat shapes are more suitable as initial configurations for the programming; larger differences between set of curvatures from room temperature and to above Tg imply much broader available final shape changes during actuation. (b) The initial moisture content can be programmed in various ways within the composite. Every defined initial MC level creates new sets of shape at different humidity conditions. Two examples with their shape sets are here illustrated for initial MCs of 3.26% (50% RH) and 22.68% (immersed). The programming allows for a multifunctional shape transformation: shapes can

only 0.78% expansion in contrast to the 2.83% at room temperature); (c) be compliant over T_g to release internal stresses and d) suitable T_g temperature for the operational requirements of the devices made with the biobased material. The matrix in this case is an epoxy based SMP provided by Leng's group [15]. The elastic modulus of the SMP matrix used here is 1.6 GPa at 20 °C, but only 20 MPa at 100 °C. The low modulus provides compliance to release the internal stresses between active and passive layers with a relatively low-temperature T_g at 60 °C. The viscoelastic properties of the shape memory polymer are shown in Fig. S1 d. The shape memory effects of the matrix allow to keep the overall original external shape of the composite, with matrix and fibres positions self-adjusting during the changes of temperature and moisture. This is a functionality that state-of-the-art hygromorphs based on natural fibres and standard matrices do not possess, because their shape change is only due to the expansion of the fibres of the active layers when internal moisture variations occur. The self-adjustment between matrix and fibres positions also allows to keep flat shapes during programming within the asymmetric bilayer structures. The expansion properties at two temperatures are verified by hygroscopic experiments at room temperature and over the T_g (Fig. S1 c). The verification is also performed via the use of a finite element model (**Fig. S2**).

2.2. The HyTemC working process for required curvatures in operational environment

In operational terms, the fundamental mechanisms for the actuation of the HyTemCs is shown in Fig. 2a. The material designer that aims at developing actuators with these biobased materials needs first to consider the operational environment (either water immersion or target operational humidity) and the set of shapes required by the actuator (step #1). Step #2 consists in the programming, which is performed by heating up to T_g, while at the same time drying or wetting the actuator made with the hygromorph composite according to the operational requirements described in step #1. Small variations of shape changes occurring during this programming step should also be considered for the design of the biobased actuators. After the programming steps, the material is cooled until room temperature is reached (step #3). Consequent shape changes of the material are obtained in an autonomous way, when the hygromorph actuator is exposed to different operational environments. In the examples shown later, our hygromorph programmable biobased materials are designed to grasp, handle and release objects by controlling the internal humidity into a shape for the next cycles. Programming for different applications is based on the initial MC level, controlled by the mass diffusion time. The materials are stored at 0% RH (heating upon 60 °C), as the reference state (MC at 0%). The targeted curvature of the actuator at any relative humidity condition and initially programmed moisture content follows the relation shown in Fig. 2b, in which the $[0_2 90_6]$ laminate is taken as an example. The two red lines in the figure indicate two sets of shapes with initial MCs of 3.26% (the curvature ranges from -13.54 m^{-1} at RH 9% to 65.06 m^{-1} in immersed condition) and 22.68% (curvature from -68.23 m^{-1} at RH 9% to 16.02 m^{-1} in immersed condition) respectively; those moisture contents provide the actuated shapes shown in Fig. 1b. Here the changes of curvature have a linear relation between the hygroscopic expansion mismatch provided by the active and passive layers, as predicted by the modified Timoshenko equation [3]. The actuating times are of the order of several tens of minutes (up to $\sim$ 150 mins – see Fig. 2c). Fig. 2d and e show the distribution of the total stresses through the thickness of the selected $[0_2 90_6]$ HyTemCs calculated via Finite Elements (FE). The case in Fig. 2d involves full immersion in water as the operational environment: the initial moisture content is programmed initially at 3.26% and the actuator absorbs water up to a maximum of 22.68% MC, reaching a curved shape. The other case (Fig. 2e) is related to an operational surrounding environment of 50% RH. Our hygromorph-based actuator with 22.68% initial MC first desorbs until the moisture content stabilizes to a value close to 4.71% (the difference 1.45% is due to hysteresis). The largest stresses of the passive and active layers occur near the interface and have opposite signs: 29 MPa in tension (positive) within the passive layers but 10 MPa in compression (negative) in the active ones (in absorption case – Fig. 2d). During desorption (Fig. 2e), the maximum stresses are 60 MPa in compression in the passive layers, but 40 MPa in tension with the active layers. The programmed initial shapes before actuation have lower stresses than during the actuation phase (all cases are lower than 10 MPa) because of the small deformations involved, no matter whether absorption or desorption occurs. Different cases of absorption or desorption generate opposite stress modes, in tension or compression. The significant stresses mismatch is due to the enhanced elastic properties of the actuators made with our bio-based hygromorphs (see Supporting Information 1e), and the plasticizing effect of water. From a material strength perspective, the stress state of the active layers is more critical than the one of the passive layers. The active layers are in compression during absorption (Fig. 2d), but under a structurally critical tensile state during desorption (Fig. 2e). The transverse strengths of the composites with MCs of 1.51 and 15.67% are 9.99 $\pm$ 1.05 MPa and 4.21 $\pm$ 0.58 MPa – (see Fig. S1 g). The calculated stresses are larger than the experimental ones, and this indicates the onset of damage that makes the curvatures degrade with the increasing numbers of cycles.

3. Results and discussion

3.1. Evaluation of the actuation performance

This section is about how to formulate the design of the programmable hygromorph biobased materials actuators based on the available design space (curvature, stiffness and actuating time), parametrized versus the thickness of the active and passive layers (Fig. 3a). The design space is explored by using modified Timoshenko equations [3]. The difference in hygroscopic expansion between the active and passive layers used here is 2.83% (from a moisture content of 0%, to one of 15.67% when immersed - Fig. S1 c). The grey area in Fig. 3a consists of laminates with extremely thinner layers and large curvatures, which are beyond the current technical scope of the laminates. The three squared markers in the Figure are related to the 0.56 mm overall thickness used in our samples with laminate stacking sequences of $[0_1 90_7]$, $[0_2 90_6]$ and $[0_3 90_5]$ from right to left, respectively. The HyTemCs have coordinate systems (1,2), traditionally used to define composite stackings (1 - longitudinal and 2 - transverse directions). Errors between experiments and analytical results are 0.6%, 3.3% and 46.3% for the three different types of laminates (Fig. 3a and d). The reason for the large discrepancy related to the $[0_3 90_5]$ materials system is related to the fact that the corresponding laminate architecture is nearly balanced; the analytical model used here is suitable for biomaterials and composites with large numbers of active layers, but small relative numbers of passive layers.

The bending stiffness is an important parameter to describe the actuation authority, i.e., the generation of large actuating forces to displace objects and locking those in a fixed configuration when the actuation is completed. All samples here have the same size (70 mm*1 mm), but different thickness. An effective bending stiffness is computed in the fixed state as a proxy to identify the holding force shown in Fig. 3b for flat shapes, and 3c for a curved configuration. The displacement of the straight beam (Δy) due to an

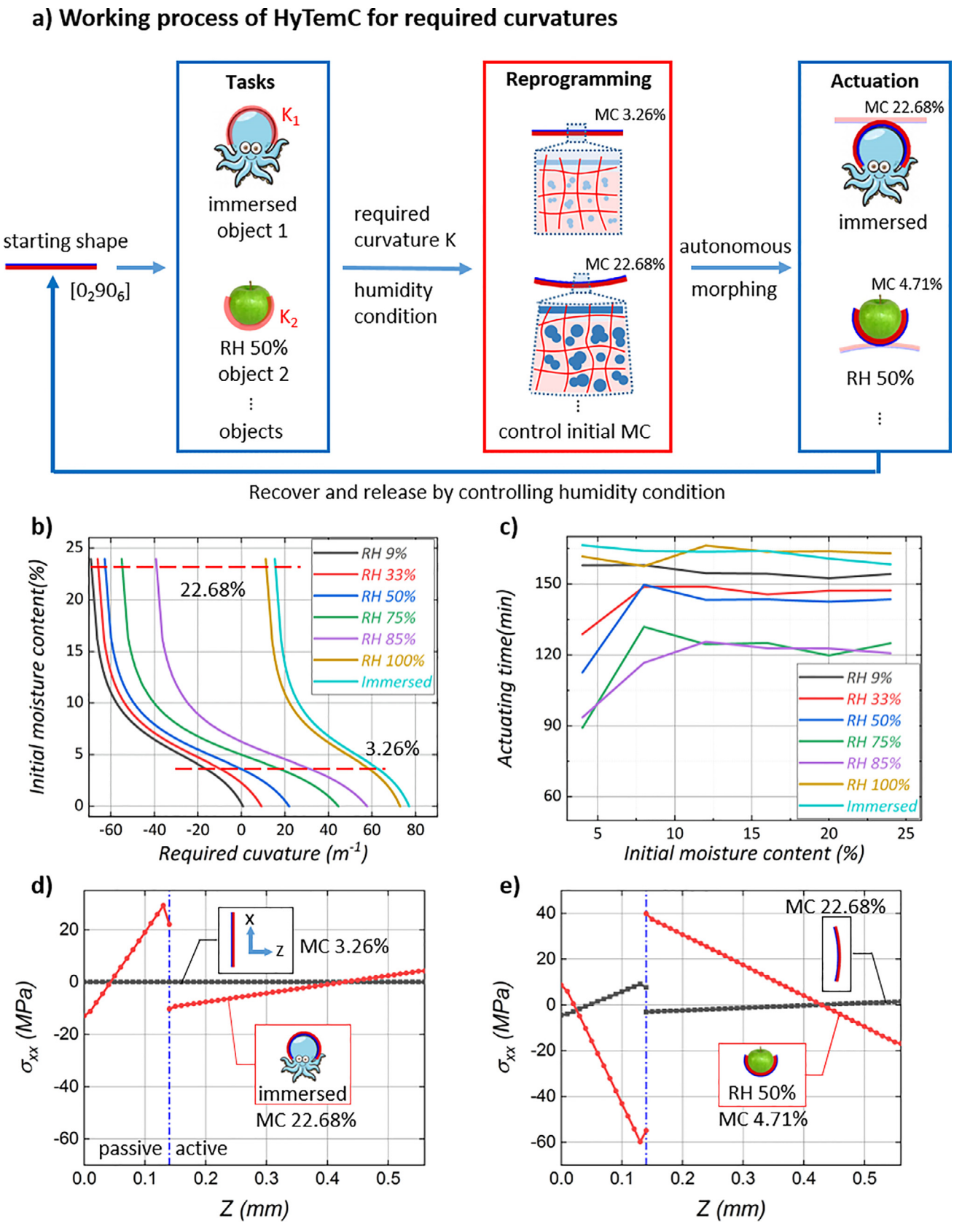

Fig. 2. (a) Actuation working process: measurement of the operational RH conditions and design of the required curvature; programming of the material to define its initial MC, while maintain the structure of the hygromorph material actuator nearly flat; final autonomous actuation within the operational RH environment. Two cases of shape transformation cycle: one sample is set with an initial MC value of 3.26%, but bends significantly and autonomoulsly when it is immersed, reaching an internal moisture content of 22.68%. The other sample is nearly flat, with an initial MC value 22.68% during programming, but bends within a RH 50% environment to reach an internal moisture content of 4.71%. (b) Designed initial moisture content levels during programming, according to operational RH conditions and required curvatures. Two redlines are displayed here for two shape sets with initial MCs of 3.26% and 22.68%; those shapes show a good agreement with those represented in Fig. 1b. (c) Actuating time of samples with initial MC levels to reach a substantial dimensional stability in various environments. Substantial stability means here a tranfer of 90% moisture with very small residual shape changes. (d) and (e) show the global stresses distributions of the hygromorph composite actuators in the longtitudal direction during absorbtion and desorption (3.26 to 22.68% and 22.68 to 4.71%).

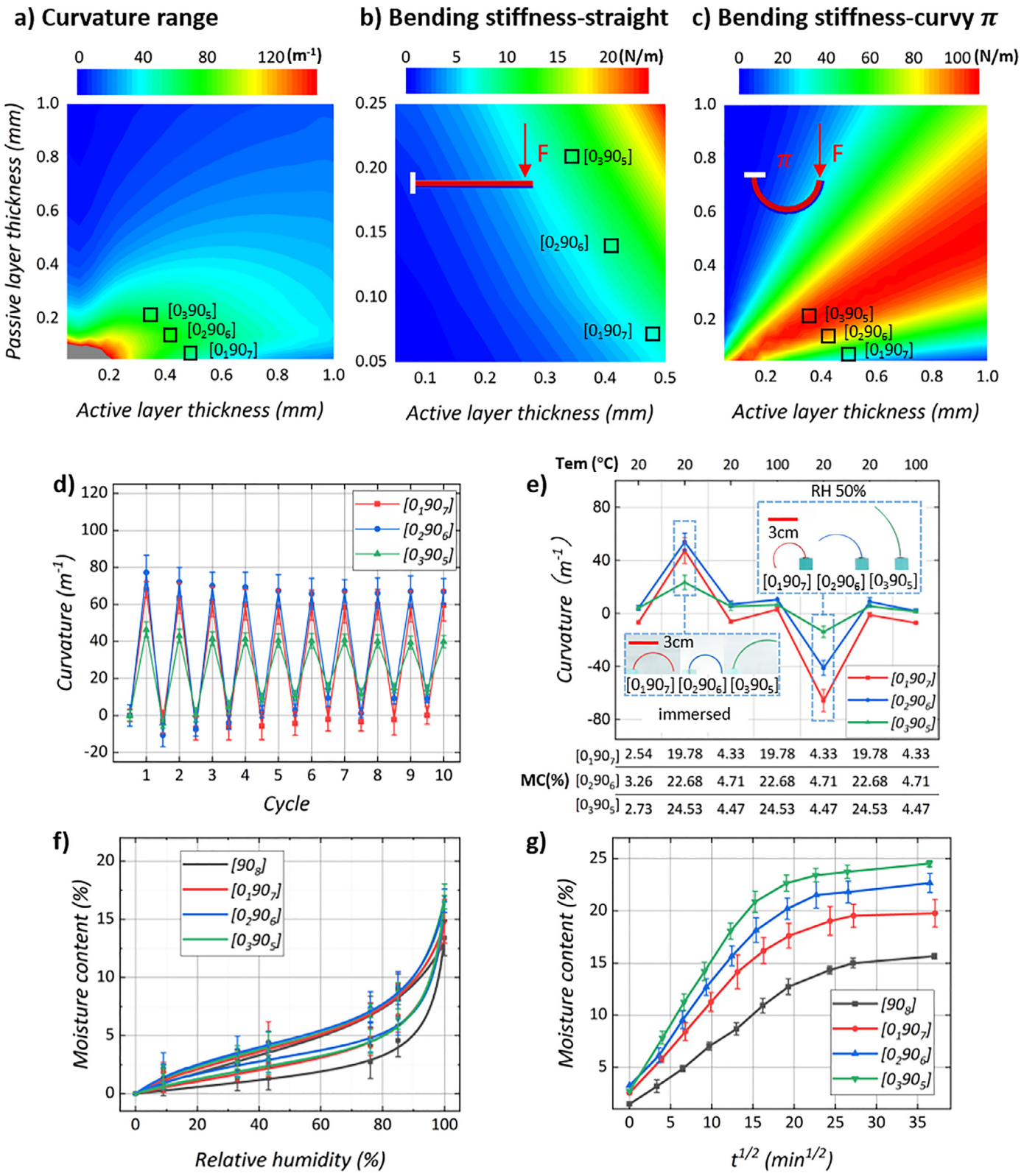

Fig. 3. Architecture design of asymmetric HyTemC considering curvature ranges, stiffness and moisture diffusion. The thickness of active and passive layers is the main driver of these three goals. (a) Curvatures as a function of the two-layer thicknesses from RH 50% to immersed states. (b) and (c) Plots of bending stiffness for flat and curved actuator (latched at π rad) versus the two types of thicknesses. The three squares are related to a 0.56 mm overall thickness, with a ratio between active and passive layers following composite stacking sequences of $[0_1,90_7]$ (38.3 N/m), $[0_2,90_6]$ (92.1 N/m) and $[0_3,90_5]$ (107.2 N/m) respectively. (d) Curvature ranges for three different laminates after 10 cycles from RH 50% to immersed states. (e) Curvature changes during the programming and actuating processes after 10 cycles. The Figure contains cases 1 and 2 together, showing the complete process to obtain required bending curvatures at different RH conditions. (f) Moisture conditions at various RHs for different laminates. Slightly differences between absorption and desorption are due to hysteresis. (g) Moisture diffusion from 50% RH to immersion. The variation of moisture content is very small within the different actuators.

external force of F can be expressed as:

$$K_{bending} = \frac{F}{\Delta y} = \frac{3EI}{l^3} \quad (1)$$

where E is the bending modulus calculated based on the D_{11} term of the bending matrix from classical laminate theory [23], l (70 mm here) is the length of the beam and I the moment of inertia. The curvature angle of the curved shapes is constant at π (180°) and taken as the reference angle to design the bio-based materials active laminates. We have used the usual form of Castigliano's energy theorem to express the curvature of this device as:

$$\Delta y = \int_0^{\pi} \left(\frac{M_{(\theta)}}{E_i I_i} \frac{\partial M}{\partial F} \right) ds \quad (2)$$

where M is the moment due to the force F, $E_i I_i$ is the equivalent stiffness of all the layers with E_i and I_i being the modulus and the area moment of inertia of i^{th} layer, respectively. The bending stiffness of this curved beam is $K_{bending} = F\Delta y^{-1}$.

In the flat shape configuration of Fig. 3b, the largest bending stiffness is obtained by adopting thick HyTemCs. A high passive thickness helps to obtain larger values of stiffness, albeit the overall thickness is here kept constant because the tensile modulus of the passive layer is at least 5 times larger than the active layer (see supplementary Fig. S1 d). This implies a trade-off between the different design parameters: a thickness increase provides larger loading bearing capabilities but lower achievable deformations during actuation, and lower reactivity due to moisture diffusion. Since the in-plane dimensions of the HyTemCs are much larger than the thickness, water diffusion mainly occurs here along the through-thickness direction.

In the case of curved shapes (Fig. 3c), the higher curvature implies a lower radius and therefore shorter material strips to achieve the same 180° final bent shape. Aside from thickness effects, shorter strips with larger curvatures have therefore more potential to bear higher loads by a geometrically induced stiffening effect. The $[0_1 90_7]$ laminate is not the optimal one in terms of actuator stiffness (38.3 N/mm), compared to the $[0_2 90_6]$ one (92.1 N/mm) (see Fig. 3c); the stiffness associated to the flat shape version is however adequate. The reason behind this is the increased number of passive layers in the $[0_2 90_6]$ configuration that leads to a larger overall bending (see in Fig. 3c the lower stiffness of the $[0_1 90_7]$ compared to the one provided by the $[0_2 90_6]$).

In a real environment, actuators with our hygromorph bio-based material systems could be subjected to cyclic variations of the moisture content. We performed cycles of immersion and desorption at 50% RH to ascertain the behavior of these materials. Despite an almost constant value of the actuated maximal curvature at wet state after 10 cycles, the different laminates exhibit a loss of curvature between wet and dry states: 87.2% ($[0_1 90_7]$), 75.0% ($[0_2 90_6]$) and 55.7% ($[0_3 90_5]$) after 10 cycles (see Fig. 3d). The $[0_3 90_5]$ laminate has a more dramatic degradation of the actuated curvature, from 46.4 m^{-1} to only 25.8 m^{-1}. Water immersion is a severe environment for natural fibre biocomposites with multiple degradation mechanisms occurring, such as fibre polysaccharide leaching, and severe modification of fibre/matrix interface. An improvement of the durability of these bio-based actuators can be however observed when using natural fibres with more lignin content (jute, for example) or by applying variations of the relative humidity, rather than immersion.

In terms of programming and actuation processes, the actuated curvature ranges are 59.5 m^{-1} $[0_1 90_7]$, 49.0 m^{-1} $[0_2 90_6]$ and 18.5 m^{-1} $[0_3 90_5]$ respectively (Fig. 3e). The programming curvature ranges are only 7.5 m^{-1} $[0_1 90_7]$, 5.5 m^{-1} $[0_2 90_6]$ and 2.5 m^{-1} $[0_3 90_5]$- see Fig. 3e. The 2.5 m^{-1} is barely detectable, especially when the shape is nearly flat. Fig. 3e also shows that the moisture content between actuators varies only a little.

Moisture diffusion properties of the HyTemCs are shown in Fig. 3f and g. The moisture content related to four types of architectures ($[90_8]$, $[0_1 90_7]$, $[0_2 90_6]$ and $[0_3 90_5]$) at various RH values are shown in Fig. 3f. The moisture content of a specific architecture at any RH condition can be calculated once the humidity environment is stabilized, even if a hysteretic behavior makes the MC during absorption slightly smaller than during desorption. A diffusion kinetics experiment has been performed (Fig. 3g). The diffusivities (10^{-6} mm/s) of the four laminates are 1.77 of $[90_8]$, 2.69 of $[0_1 90_7]$, and 2.70 of $[0_2 90_6]$ and 3.46 of $[0_3 90_5]$. The actuating speeds are similar because of the similar diffusion coefficients.

In summary, the $[0_2 90_6]$ architected bio-based hygromorph actuator with two passive layers possesses overall satisfactory properties in terms of stiffness and final curvature, and it will be considered as the baseline for the activities further described in this work.

3.2. Examples of prototypes

Two applications of the HyTemC are here demonstrated: a gripper with five fingers working in both the water and air, and smart frames for an electro-adhesive structure. Application #1 displays similar curvature shapes at different RH conditions (50% and immersion), a feature that is not available in current hygromorph composites [3,21]. Also, various shapes at the same RH condition (50% RH) are shown for application #2. These two examples show the characteristics of the HyTemC, like autonomous actuation without external power supply, programmable actuated shapes and reversible and repeatable actuation. Remarkable stiffness properties also allow the lifting of heavy objects in Application #1, and adjustable motions when operating with structures within constrained spaces (see Application #2).

3.2.1. Gripping objects in the water and air

To illustrate the augmented functionality and versatility provided by actuators made with our HyTemCs, we designed a five-fingers gripper to pick objects in water and air (Fig. 4a and Video SV1).

The gripper has at first 5 HyTemC stripes. Case #1 of the application of the gripper is to grasp a 60 mm (curvature $K = 33$ m^{-1}) diameter ball immersed in water. The operational humidity condition is immersion, and the required curvature is 60 m^{-1}; large curvatures help grasping heavier objects because of the larger friction between the material and the objects themselves. From the design map of Fig. 2b, the programmed initial moisture content level should be 3.26%. We followed a similar method also for case #2, with operational RH of 50% and same required curvature 60m^{-1}, so that the programmed initial MC level for this case is 22.68%. The process to set the initial MC levels involves heating upon 100 °C over the Tg temperature and then dry or wet the material until the desired moisture content is achieved. The device flips from orange/white to white/orange because of the opposite bending directions. After transferring the ball to other locations, the release of the ball itself is done via moisture absorption or desorption of the hygromorph stripes induced by a modification of the environment. The actuating speed in water is faster than in air because moisture desorption is slower than absorption, as similarly observed in other works [3].

The high stiffness provided by our HyTemC makes it possible to carry relatively heavy objects, even several times heavier than the weight of the 5 stripes gripper alone. The exact lifting force in water is difficult to be assessed because of the buoyancy and additional added mass to the ball. In the air, our 2.8 g (5 stripes

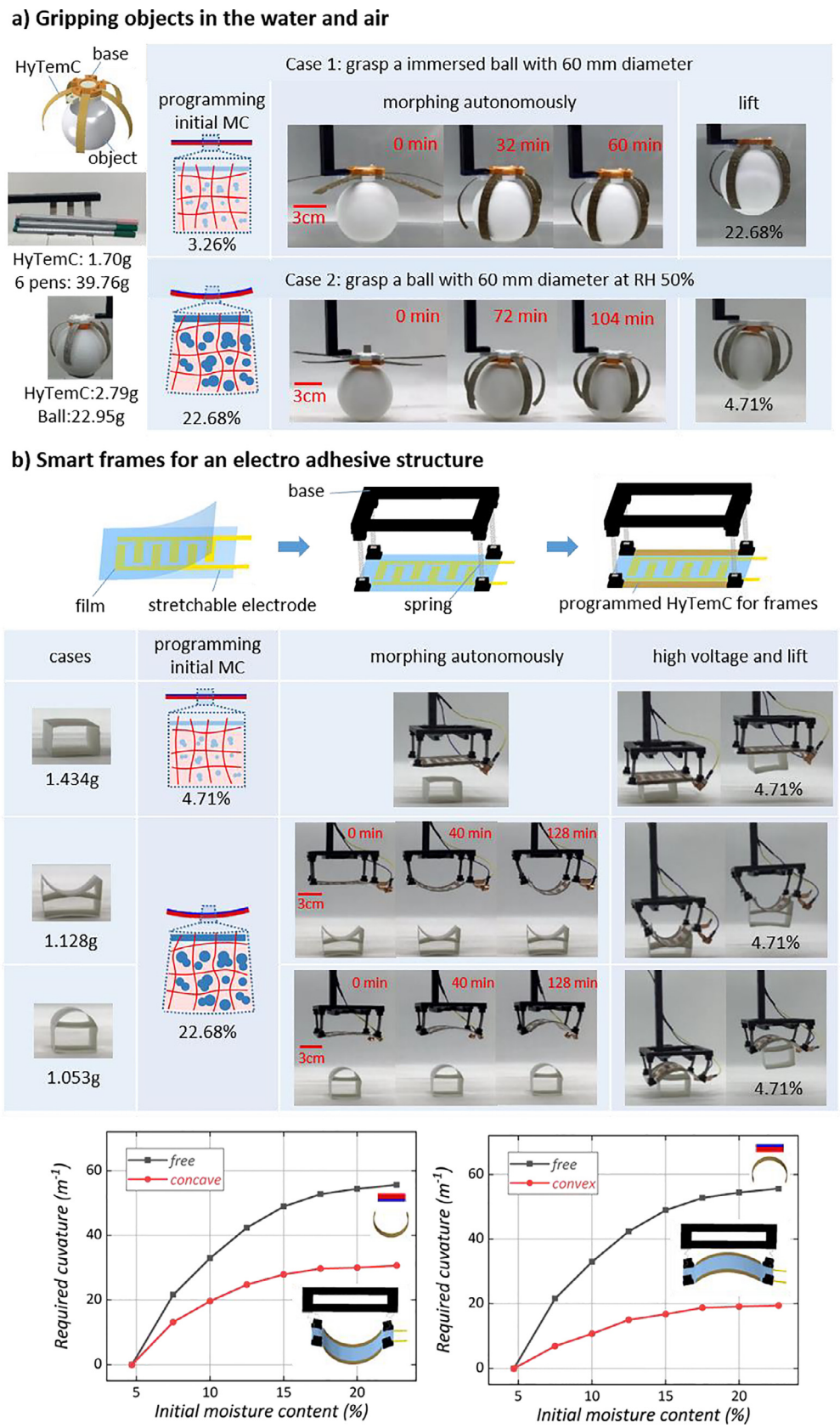

Fig. 4. (a) Gripping objects in water and air. The design of the grasping structure consists of a stiff base and five connected strips of our hygromorph bio-based laminates. The evolution of the shape in water and air (RH = 50%) is displayed. The maximum lifting weight of the ball is around 2.3 g in the air condition, while the five strips are only 2.8 g. 3 strips can hold six pens at ease with around 40 g weight in the air condition. (b) Smart frames for electroadhesive structure. Manufacturing process of the adhesive structure: stretchable electrodes are deposited in the insulated Mylar film, which is bonded to the HyTemC. The film is connected to a stiff base via four springs. The evolution of the shapes to conform to the objects surfaces is shown here. This adaptive structure can bond flat, concave, and convex surfaces at room environment. The maximum lifting weight for the three conditions are 1.434, 1.128 and 1.053 g. The relationships between the required concave and convex curvatures and initial MCs are given in the charts. (a) shows similar shapes in the air and water while (b) presents various shapes for the same RH condition.

overall) device however manages to hold the 23 g ball easily, although the shape of the ball is quite complex to grasp. The device could also be capable to carry larger weights at ease, by changing - for example - the ball with a cylinder, or by adding some grooves that facilitate the grasp. Three HyTemC stripes of 1.70 g can lift six pens (≈40 g); this corresponds to 23 times their own weight. This example confirms the ability of our materials system to be used for force generation, similarly as a natural hydraulic actuator (e.g., the pinecone). However, our materials system can provide load bearing capacity and adjustable working conditions (immersed, or RH 50% normal room humidity), by following the programming method developed in this work.

3.2.2. Smart frame for an electro adhesive structure

The previous application has shown that these HyTemCs can also be used as components within a structural and load-bearing configuration. To this extent, an adaptive electro adhesive structure has been designed to be used as a smart frame. If the upper part of the structure is the active layer, the actuated shape is convex. An inverted architecture with the upper passive layer will generate a concave shape, although the programming moisture comments are both at 22.68%. A pair of conducting electrodes can be deposited on one side of the structure. An induced electro-adhesive force is developed at the electrodes by applying high voltage that attracts objects to the gripper. The structure can change its curvature to match different shapes (Fig. 4b). The 90 mm * 70 mm size film used here can bond to ~1.40 g flat-surface objects with 5KV voltage of input. In our case, the setting directions of the laminates made with the HyTemCs can be designed into active layers facing up or down. We can therefore decide in this way to generate either adhesive convex or concave surfaces. Various surface configurations can be created (flat, concave, and convex) by making the film and the spring to interact together. Our materials overcome the limitations of traditional humidity-induced response composites by actuating at dry state until the conformal shapes are obtained, and then activating an electric circuit to bond objects.

A curvature loss is however observed, likely due to the compliance and partial inelasticity of the springs. At 20 °C, our HyTemCs also become soft with a high moisture content and their behavior can be easily affected by boundary/edge effects during the actuation. The curvature therefore assumes a value of 39.3 m^{-1} when the device is bent to match the concave surface – the analogous value predicted by the FE model is 30.6 m^{-1}. When the convex surface is matched, the same type of curvature is however 26.7 m^{-1} (19.4 m^{-1} in the FE model). The relations between initial MCs and predicted curvatures of the concave and convex surfaces are conservative compared to the experimental values, and this feature could be used as a baseline design approach for the programming and design of the HyTemCs electro adhesive systems.

4. Conclusion

Classical hygromorph composite materials provide large responsiveness, good mechanical properties, autonomous actuation and low-carbon environmental impact. However, classical hygromorphs feature a limited one-way relation between surrounding relative humidity and the curvature of the actuator devices made from those materials. The present work proposes novel programmable hygromorph biobased materials systems using shape memory polymer matrices to produce actuators that provide various fixed and resettable bending shapes at constant RH environment, by combining thermal and moisture stimulus at programming and actuation levels. The thermal programming method makes these proposed materials work at both room humidity and water and at different designed curvatures.

The hygromorph biobased material systems proposed here possess the following qualities:

- Autonomy: the actuating process is autonomous. Existing smart responsive materials require extra devices to provide the stimulus needed for the actuation. Piezoelectrics and electroactive polymers are dependant on electronic integration [9–12], while pneumatics and hydraulics rely on pumps to force the dynamic reconfiguration of the fluids [13,14]. Shape memory materials (polymers and alloys [15,16]) typically require the immersion or contact with hot air/gas flow [6], hot liquid [17] or being actuated by electrothermal films [18]. As a contrast, the HyTemCs are stimulated by the surrounding humidity and thermal environments, and do not require extra devices to improve their adaptability in limited conditions.
- Wide operational environment: the designed shapes can be programmed and generated under any humidity condition. The HyTemCs can be programmed in advance according to different operational environments to obtain a required actuation, while existing hygromorph composites [3,21] are limited to only one shape at a constant humidity level. The HyTemCs shown in this work can offer a material platform to design grasping devices in both water and air with different programming steps that broaden their operational capability.
- Generated stresses: The comparative actuation stresses are shown in Fig. 5, and the values of other materials are from the other work [24]. The generated actuation stress is calculated from the transverse hygroscopic expansion and the longitudinal stiffness. The generated stresses are 20.2 MPa actuating from RH 50% to immersed but 88.6 MPa from immersed to RH 50%, corresponding the lowest point and the highest point of purple area in the Fig. 5. The difference is because HyTemCs display higher mechanical properties at RH 50% than when in immersed state. The actuation stress of the HyTemCs is larger than more established smart materials (like SMPs, EAPs and partially SMAs); amongst natural fibres hygromorph composites [21], the HyTemCs provide a broader actuation envelope because of the above mentioned wide operational environment, which allows the generation of different actuation stresses.
- Repeatability: actuation and programming could be repeatable without any external force. Degradation is observed with cycles of changing curvatures from RH 50% to the immersed state, however these hygromorphs show stability after 5 cycles (Fig. 3d).
- Load bearing characteristics and actuation authority: our HyTemCs have significant mechanical properties (tensile modulus of 13.8 GPa in the longitudinal and 3.5 GPa along the transverse directions at 20 °C and RH 50%). Those values are much larger than popular pure shape memory polymers, dielectric elastomer made by silicone (1 MPa) [25], and acrylic (2 MPa) and electroactive polymers (0.1 and 1 GPa) [26]. Our bio-based hygromorphs feature values 13 times larger in longitude and 3 times bigger in the transverse direction.
- Shape stability: after actuation, the device made with our materials system maintains the actuated shapes (zero-power).
- Easy to make and environmentally friendly: the manufacturing method is easy and based on traditional resin film infusion techniques for autoclave, rather than complex chemical synthesis. Additionally, flax technical fibres are relatively inexpensive and recyclable. The flax prepreg tapes with shape memory polymers are readily accessible and can be applied widely at laboratory and industrial scales for applications involving autonomous actuations using sustainable materials.

The drawback is represented by the actuation time of the devices made with our hygromorph biobased materials systems. Future work will aim to improve the speeds of moisture ab-

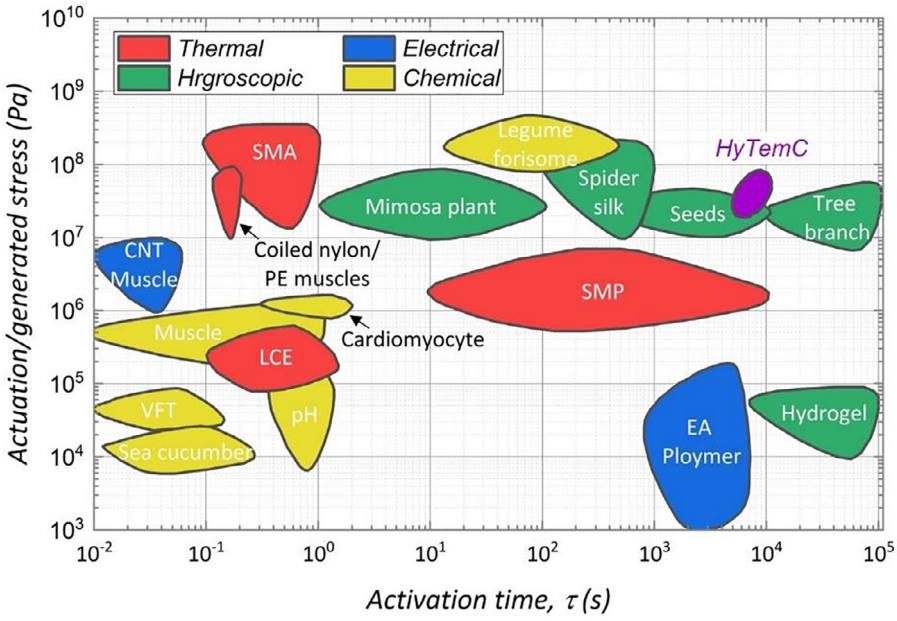

Fig. 5. Actuation/generated stress (defined as the stress generated when the material undergoes some defined actuation) and their activation time (time required to complete an actuation cycle) [24]. Materials are classified by color in terms of the mechanism of their activation and include chemical (yellow) electrical (blue), hygroscopic (green) and thermal (red) passive mechanisms. Our HyTemC is represented in purple. The generated stresses are 20.2 MPa actuating from RH 50% to immersed, and 88.6 MPa from immersed to RH 50%. The stress values are comparable to those provided by SMAs and other biobased materials like mimosa plants and spider silk. The unique programming feature of HyTemCs allows however an actuation from immersed to RH 50% with larger stresses than other hygroscopic natural materials, although the actuation stress from RH 50% to immersed is like those from natural plant-based solids, for example.

sorption/desorption by increasing the fibre volume fraction, by 4D printing/additive manufacturing thinner hygromorph laminates that reduce the water transport distance and enhance the moisture behavior of the shape memory epoxy used in this concept.

5. Experimental section

5.1. Material supplier and processing

Unidirectional flax fibre tapes (50 g/m^2) were supplied by Natup. Pure flax fibres are fixed by tape on their boundaries and cut into 250 mm*250 mm size. Stacks of epoxy films and unidirectional flax-fibre tapes (50 g/m^2) have been cured in autoclave with 0.69 MPa pressure heating for 80 °C 3 h, 100 °C 3 h and 150 °C 5 h. The thickness of the active and passive layers is determined by using a classical laminate theory approach mixed with modified Timoshenko beam formulation which predicts the final curvature and stiffness of the hygromorphs [3,21]. We use an 8-layer flax tape overall. The passive and active layer ratios are $[0_1 90_7]$, $[0_2 90_6]$ and $[0_3 90_5]$, respectively. The composite plates are cut into small stripes of 70 mm in length and 10 mm in width.

5.2. Sample storage

All samples are stored in a sealed bag at room temperature (23 °C) around 70% RH before use. During the experiments the hygromorph biobased plates have been stored in chambers with relative humidity (RH) controlled by a saturated solution of potassium hydroxide (KOH), magnesium chloride ($MgCl_2$), potassium carbonate (K_2CO_3), sodium chloride (NaCl), and potassium chloride (KCl) so as to reach RH values of 9%, 33%, 44%,75%, and 85%, respectively. The 50% RH conditioning has been performed using a Votsch climatic chamber which controls RH and temperature together. Samples were used after reaching saturation, i.e., when the weight was stabilized, and more than 48 h should be the safe time.

5.3. Diffusion experiment

Unidirectional and asymmetric laminates were stored at 50% RH and 23 °C to allow the attainment of the reference state. The materials were then immersed in deionized water at room temperature. During immersion, the samples were periodically removed to be weighed (using a balance with an accuracy of 10^{-3} g) and characterized. The percentage gain C (MC) at time t is calculated as:

$$C_{(t)} = \frac{W_t - W_0}{W_0} \cdot 100 \quad (3)$$

where W_t and W_0 are the weight of the sample at time t after water exposure and the weight of the dry material before immersion (for RH = 50% and T = 23 °C), respectively. The maximum moisture absorption C_s is calculated as the average value of five consecutive measurements where each measurement has been performed on 5 samples and averaged arithmetically.

5.4. Expansion measurement

Hygroscopic expansion and moisture uptake have been evaluated on samples 70 mm (L) × 10 mm (w) × 0.56 mm (t). The size is the same as the real used samples. Volumetric measurements have been performed with a Mitutoyo micrometre IP65 and gravimetric analyses using a Fischer Scientific PAS214C balance (10^{-3} g). The coefficient of hygroscopic expansion (β) was determined as the slope of the hygroscopic expansion over the MC. The results are shown in Supplementary Information.

5.5. Elastic properties

The tensile properties of dry and wet unidirectional biocomposites with flax fibre orientation set at 0° (E_L) and 90° (E_T) were measured separately according to ISO 527-4 standards, using a Shimadzu universal testing machine (cell load 5 kN) at controlled temperature (23 °C) with a crosshead speed of 1 mm/min. The

samples have the following dimensions (thickness t and width w): $t_{0°}$=0.56 mm and width $w_{0°}$ = 15 mm; $t_{90°}$=0.56 mm and $w_{90°}$= 25 mm. Mechanical tests were performed on samples that had reached their saturation time. The samples were wrapped with polymer film to prevent the loss of moisture. A heating chamber to control setting temperature and thermocouples were also used to verify the temperature near the samples. An axial extensometer with a nominal length of 25 mm (L_0) was used to measure the strain. The tensile modulus was determined within a range of strains between 0.05 and 0.1%.

5.6. Measurement of the curvature

To measure the radius of curvature, markers were tracked on the images captured using a camera (1080P HD, 30fps). and image analysis was performed using Autodesk software. The curvature was measured by fitting the time history of the sample profile to a 'circle' function. The bending curvature (K) was calculated with the radius of the fitted circle.

5.7. Maximum lifting weight measurement

The lifting objects are balls and pens for the grasping hand and flat, concave and convex shapes for the electroadhesive structures. We have tied Blue Tack (adhesive putty) on the objects to adjust the overall weights, which have been measured using a Fischer Scientific PAS214C balance (10^{-3} g).

5.8. Prototypes manufacturing

Insulated Mylar film have been used as the adhesive face to bond to the hygromorph devices. The films have a 0.075 mm thickness and were procured from RS Components UK. The same supplier provided a stretchable electrode with 8 mm in width and 0.07 thickness. The electronic circuitry was protected by a modified polyurethane coating (amber). The film was combined with a stiff base through four low stiffness stainless steel springs (spring constant of 0.16 N/mm, outside diameter 3.52 mm and free length 29.3 mm). The operational voltage was 5KV, provided by an adjustable power supply and EMCO that can boost voltage 1000 times.

Declaration of Competing Interest

The authors declare that they have no known competing financial interests or personal relationships that could have appeared to influence the work reported in this paper.

CRediT authorship contribution statement

Qinyu Li: Conceptualization, Methodology, Software, Investigation, Writing – original draft, Visualization. **Rujie Sun:** Conceptualization, Validation, Formal analysis, Writing – review & editing. **Antoine Le Duigou:** Resources, Writing – review & editing, Supervision. **Jianglong Guo:** Conceptualization. **Jonathan Rossiter:** Conceptualization, Writing – review & editing. **Liwu Liu:** Resources, Writing – review & editing. **Jinsong Leng:** Resources, Writing – review & editing, Supervision. **Fabrizio Scarpa:** Resources, Writing – review & editing, Supervision, Project administration, Funding acquisition.

Acknowledgments

Authors 1 and 2 contributed equally to this work. QL is grateful for the support of the Faculty of Engineering of the University of Bristol. FS acknowledges the logistical support of the H2020 BBI SSUCHY project for the use of the flax fibres and the composites manufacturing facilities. FS also acknowledges the support of the ERC-2020-AdG 101020715 NEUROMETA project.

Data availability statement

The data that supports the findings of this study are available in the Supplementary Information of this article

Supplementary materials

Supplementary material associated with this article can be found, in the online version, at doi:10.1016/j.apmt.2022.101414.

References

[1] E. Hawkes, B. An, N.M. Benbernou, H. Tanaka, S. Kim, E.D. Demaine, D. Rus, R.J. Wood, Programmable matter by folding, Proc. Natl. Acad. Sci. 107 (2010) 12441–12445, doi:10.1073/pnas.0914069107.
[2] J. Mu, C. Hou, H. Wang, Y. Li, Q. Zhang, M. Zhu, Origami-inspired active graphene-based paper for programmable instant self-folding walking devices, Sci. Adv. 1 (2015) e1500533, doi:10.1126/sciadv.1500533.
[3] A.Le Duigou, G. Chabaud, F. Scarpa, M. Castro, Bioinspired electro-thermo-hygro reversible shape-changing materials by 4D printing, Adv. Funct. Mater. 1903280 (2019) 1–10, doi:10.1002/adfm.201903280.
[4] L. Hines, K. Petersen, M. Sitti, Inflated soft actuators with reversible stable deformations, Adv. Mater. (2016) 3690–3696, doi:10.1002/adma.201600107.
[5] J. Kim, S.E. Chung, S. Choi, H. Lee, J. Kim, S. Kwon, Programming magnetic anisotropy in polymeric microactuators, Nat. Mater. (2011) 10, doi:10.1038/nmat3090.
[6] M. Behl, K. Kratz, J. Zotzmann, U. Nöchel, A. Lendlein, Reversible bidirectional shape-memory polymers, Adv. Mater. 25 (2013) 4466–4469, doi:10.1002/adma.201300880.
[7] Y. Kim, H. Yuk, R. Zhao, S.A. Chester, X. Zhao, Printing ferromagnetic domains for untethered fast-transforming soft materials, Nature 558 (2018) 274–279, doi:10.1038/s41586-018-0185-0.
[8] S. Wu, Q. Ze, R. Zhang, N. Hu, Y. Cheng, F. Yang, R. Zhao, Symmetry-breaking actuation mechanism for soft robotics and active metamaterials, ACS Appl. Mater. Interfaces 11 (2019) 41649–41658, doi:10.1021/acsami.9b13840.
[9] S.D. de Rivaz, B. Goldberg, N. Doshi, K. Jayaram, J. Zhou, R.J. Wood, Inverted and vertical climbing of a quadrupedal microrobot using electroadhesion, Sci. Robot. 3 (2018) eaau3038, doi:10.1126/scirobotics.aau3038.
[10] H. Peng, J. Yang, X. Lu, P. Zhu, D. Wu, A lightweight surface milli-walker based on piezoelectric actuation, IEEE Trans. Ind. Electron. 66 (2019) 7852–7860, doi:10.1109/TIE.2018.2883269.
[11] H. Zhao, A.M. Hussain, M. Duduta, D.M. Vogt, R.J. Wood, D.R. Clarke, Compact dielectric elastomer linear actuators, Adv. Funct. Mater. 28 (2018) 1804328, doi:10.1002/adfm.201804328.
[12] S. Gu, S. Guo, L. Zheng, R. An, Turning Locomotion Analysis and Performance Evaluation for a Spherical Underwater RobotPublisher: IEEECite ThisPDF, in: IEEE International Conference on Mechatronics and Automation, IEEE, 2019, pp. 2507–2511, doi:10.1109/ICMA.2019.8816270.
[13] M. Schaffner, J.A. Faber, L. Pianegonda, P.A. Rühs, F. Coulter, A.R. Studart, 3D printing of robotic soft actuators with programmable bioinspired architectures, Nat. Commun. 9 (2018) 878, doi:10.1038/s41467-018-03216-w.
[14] M. Wehner, R.L. Truby, D.J. Fitzgerald, B. Mosadegh, G.M. Whitesides, J.A. Lewis, R.J. Wood, An integrated design and fabrication strategy for entirely soft, autonomous robots, Nature 536 (2016) 451–455, doi:10.1038/nature19100.
[15] J. Leng, X. Wu, Y. Liu, Effect of a linear monomer on the thermomechanical properties of epoxy shape-memory polymer, Smart Mater. Struct. 18 (2009) 95031, doi:10.1088/0964-1726/18/9/095031.
[16] F. Falk, A New Constitutive Equation for Superelastic Deformation and Prediction of Martensite Volume Fraction in Titanium-Nickel-Cupper Shape Memory Alloy, Acta Metall. 28 (1980) 1773–1780, doi:10.1016/0001-6160(80)90030-9.
[17] D.H. Wang, L.S. Tan, Origami-inspired fabrication: self-folding or self-unfolding of cross-linked-polyimide objects in extremely hot ambience, ACS Macro Lett. 8 (2019) 546–552, doi:10.1021/acsmacrolett.9b00198.
[18] H. Wei, X. Cauchy, I.O. Navas, Y. Abderrafai, K. Chizari, U. Sundararaj, Y. Liu, J. Leng, D. Therriault, Direct 3D printing of hybrid nanofiber-based nanocomposites for highly conductive and shape memory applications, ACS Appl. Mater. Interfaces 11 (2019) 24523–24532, doi:10.1021/acsami.9b04245.
[19] L. Huang, R. Jiang, J. Wu, J. Song, H. Bai, B. Li, Q. Zhao, T. Xie, Ultrafast digital printing toward 4D shape changing materials, Adv. Mater. 29 (2017) 1605390, doi:10.1002/adma.201605390.
[20] J. Tamaru, T. Yui, T. Hashida, Autonomously moving pine-cone robots: Using pine cones as natural hygromorphic actuators and as components of mechanisms, Artif. Life 26 (2020) 80–89, doi:10.1162/artl_a_00310.
[21] A.Le Duigou, S. Requile, J. Beaugrand, F. Scarpa, M. Castro, Natural fibres actuators for smart bio-inspired hygromorph biocomposites, Smart Mater. Struct. 26 (2017) 125009, doi:10.1088/1361-665X/aa9410/.
[22] S.E. Bakarich, R. Gorkin, M.I.H Panhuis, G.M. Spinks, 4D Printing with Mechanically Robust, Thermally Actuating Hydrogels, Macromol. Rapid Commun. 36 (2015) 1211–1217, doi:10.1002/marc.201500079.

[23] R.M. Christensen, LAMINATES, Mechanics of Composite Materials, Courier Corporation, 2012.
[24] P. Egan, R. Sinko, P.R. LeDuc, S. Keten, The role of mechanics in biological and bio-inspired systems, Nat. Commun. 6 (2015) 1–12.
[25] Z. Suo, Theory of dielectric elastomers, Acta Mech. Solida Sin. 23 (2010) 549–578, doi:10.1016/S0894-9166(11)60004-9.
[26] K.J. Kim, M. Shahinpoor, Ionic polymer–metal composites: IV. Industrial and medical applications, Smart Mater. Struct. 12 (2003) 65–79, doi:10.1088/0964-1726/12/1/308.